EFFECT OF SOIL NAILING ON THE SLOPE STABILITY OF ROAD EMBANKMENTS UNDER TRAFFIC LOAD USING THE OPTIMIZED LEM

Amr M. Rashad[1,*], Mostafa D. Hashem[2], Afaf Abdel-Halim Mahmoud[2], Tarek Elsayed Mahmoud[1, 3]

[1]Civil Engineering Dept., Faculty of Engineering, Nahda University, Bani-Sweif, Egypt

[٢]Civil Engineering Dept., Faculty of Engineering, Minia University, Al-Minia, Egypt.

[٣]Civil Engineering Dept., Faculty of Engineering, Helwan University, Cairo, Egypt.

*Corresponding author {amr.mansour.rashad@gmail.com}

Abstract: - Road embankments may fail without warning, with devastating results. Thus, it is essential to understand the slope stability mechanism of road embankments under traffic load and optimize mathematical models of slope stability to enhance the computation of safety factors and the position and shape of the slip surface. This study's main aim is to examine the effect of soil nailing on the applicability of optimized mathematical models of the slope stability of road embankments under traffic load. Mathematical analysis was conducted using SLOPE/W software, which is based on the theories and principles of the limit equilibrium method (LEM) and enhances its results using an optimization function. The effect of Soil nailing on the applicability of optimized mathematical models of the slope stability was studied in terms of inclination, spacing, and length of the case study slope, located at Salmona village in Akhmim city, Sohag governorate for the head regulator of Nag Hamady canal. The results indicate that the optimized LEM enhanced the value of the safety coefficient in all cases considered by this study, and also modeled the slip surface's shape and position more realistically. Additionally, when the length of the soil nails and number of rows increased, the factor of safety (FOS) also increased: the proper inclination of the soil nails determined in this study was 10° to 20°.

1. Introduction

Slope stability results from a balance between driving forces that promote downslope movement and resisting forces that react to driving forces and deter movement. Slope instability arises when the resisting forces cannot balance the driving forces   and may be caused by the weight or slope of the embankment or by the traffic load on the road [1]. The displacement of soil or rock has a wide range of destructive effects on roads, tunnels, water and sewage pipes, and even structures. Sliding and instabilities can damage or block arterial roads, decrease road performance, and generally reduce the safety of the roads.

Slope stabilization techniques can be used to control slope instability. Soil stabilization refers to the process of changing natural soil to meet engineering requirements through physical, chemical, and biological adjustments. These techniques can increase the weight-bearing capacity and performance of in-situ soil and sand [2]. Soil nailing has been widely used to upgrade side slopes as a slope stabilization technique [3]–[5], because of its low cost, simplicity, and speed of construction[6].

The analysis of slope stability includes determining the mechanical properties of the soil, as well as the

shape and position of potential failure surfaces. The limit equilibrium method (LEM) has been the most-used technique to solve geotechnical engineering problems for many decades. By establishing the appropriate soil characteristics and slope geometry [7], stability calculations are conducted to ensure that the driving forces to slope failure are significantly less than the resisting forces. These calculations include calculating the factor of safety (FOS) using the LEM [8].

The ordinary method, developed by Fellenius [9], was the first method for a circular slip surface, and Bishop introduced a new relationship to the base normal force [10], [11]. Consequently, the FOS equation became nonlinear. Janbu [12] developed a simplified method for noncircular failure surfaces to divide a potential sliding mass into several vertical slices [13], [14]. Several authors have presented calculation methods for slope stability based on the limit equilibrium [15], [16]. The Morgenstern–Price procedure [17] is a general method of slices based on the limit equilibrium in which the equilibrium of forces and moments acting on individual blocks must be satisfied [18]. In the LEM analysis, the Morgenstern–Price procedure is preferred because it meets all static equilibrium requirements [19] and is more well behaved than other computational algorithms in the slope stability field [18].

Slope stability analysis has become much easier using software packages and mathematical modeling. Mathematical modeling has been used to predict some natural behaviors in various fields, including social science, medicine, and engineering [20]. In civil engineering, mathematical modeling is now prominent in almost all design and analysis work [21]. Several powerful design software packages for slope stability analysis have been developed. In this study software from GEO-SLOPE International Ltd, SLOPE/W Version 9 (2018) R2, is applied [22]. This software is based on the LEM's theories and principles.

Recently, many studies have explored the possibility of incrementally altering portions of the slip surface to improve and enhance the LEM's results [23]–[26]. The critical slip surface can be refined by iteratively altering parts of it in a process referred to as slip surface optimization, using the optimization function in SLOPE/W.

The optimization function in SLOPE/W is based on two theories developed by Greco [23] and Husein Malkawi [27], wherein the critical slip surface is optimized using a Monte Carlo method. The mathematical formulation of the solution changes slightly between the two methods, but the position of the critical slip surface is the same for both.
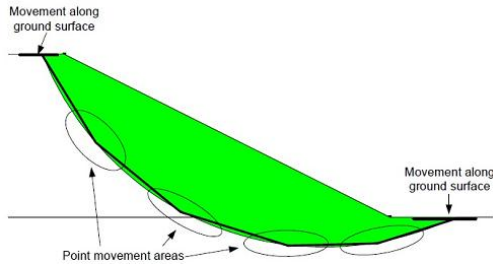
Fig. 1 Movement areas of each point in the optimization procedure[22].

As shown in Fig. 1, the optimization process in SLOPE/W begins by dividing the critical trial slip surface into several straight line segments. The number of endpoints determines the number of line segments. The vertices of each segment are then relocated in a Monte Carlo-based statistically random routine within an adjacent elliptical search area to find an existing lower FOS.

Because the user also specifies the number of starting points, this option, including the number of endpoints, controls how the optimized slip surface can deviate from the circular slip surface from which it is constructed. A significant number of starting points produces a starting slip surface composed of straight line segments that more closely approximates a

circular slip surface, as it can more closely follow the circular arc [22].

As shown in Figure 2, mathematical functions are utilized in the xy-plane to describe the topography of the soil layers, the slip surface, and the water table. To describe the geometrical boundaries, Greco [23] and Malkawi [27] use the same functions. The geometrical boundaries seen in Figure 2 are described by Equations 1, 2, 3, 3, and 5: the soil's topographic profile, the discontinuity surface in layered soils, the lower boundary, the slip surface, and the water table.
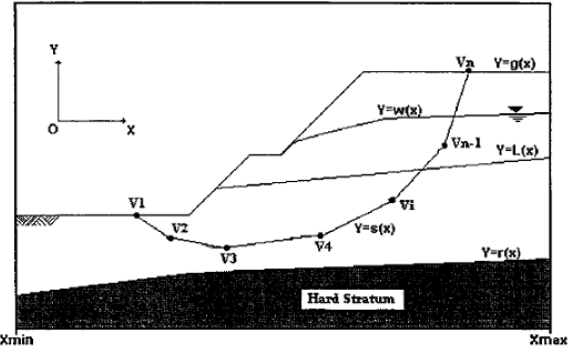
Fig. 2 The slip surface line is expressed by its vertices, while geometric boundaries are expressed by functions [27].

$$Y = g(x) \qquad (1)$$

$$Y = L(x) \qquad (2)$$

$$Y = r(x) \qquad (3)$$

$$Y = s(x) \qquad (4)$$

$$Y = w(x) \qquad (5)$$

The investigation for the critical slip surface is separated into two stages: exploration and extrapolation. As illustrated in Figure 2, the slip surface is divided into n-1 straight line segments and described by n vertices $[V_1, V_2, \ldots, V_n]$ with coordinates $(x_1, y_1), (x_2, y_2), \ldots (x_n, y_n)$ [27]. The coordinates are the function's unknown variables that describe the slip surface. The optimization involves searching for the coordinates that correspond to the minimum value of the same function using Monte Carlo random walking displacement [23].

Based on the previous slip surface, the random walking method generates a new one. The $i\,th$ slip surface is modified and used as a base for the $i + 1$ for the slip surface. The slip surface is mathematically described by coordinates in a $2n$-dimensional array in the xy-plane,$s(x)$ [27] as illustrated in Equation 6.

$$S = [x_1, y_1, x_2, y_2, \ldots, x_n, y_n]^T \qquad (6)$$

As shown in Equation 7, the optimization consists in reducing the factor of safety that corresponds to the vector S, the function $F(S)$. The optimization process follows the pattern indicated in Equation 8 as the problem is solved repeatedly [23].

$$\min F(S) \qquad (11)$$

$$F(S^0) > F(S^1) > \ldots > F(S^K) > F(S^{K+1}) > \ldots (12)$$

Several authors have examined the effect of the optimization function in SLOPE/W to obtain a low FOS value as well as the position and shape of the slip surfaces more realistically. Reference [26] is limited to using the optimization function on the slope stability of road embankments under traffic load, and [28] uses the optimization function to analyze three characteristic geometries: one horizontal, one elongated, and one steep slope, with the load, applied on embankments.

This paper is organized as follows. Section ٢ describes the mathematical modeling procedure. Section ٣ presents the mathematical results and discussion. Finally, Section ٤ concludes the work.

2. Mathematical modeling procedure

Slope stability analyses can be conducted using either deterministic or probabilistic input parameters. SLOPE/W can use many soil models to model heterogeneous soil types, complex stratigraphic and slip surface geometry, and variable pore-water pressure conditions.

In a previous study, a slope failure occurred on the road's left slope after the winter closing period, when cracks formed in the asphalt road because of the difference in water levels between the two adjacent canals and the weakness of the road soil. The highway side slope failure occurred at Salmona village in Akhmim city, Sohag governorate, at (69.6 and 70.37) km, for the head regulator of Nag Hamady channel [29]. This study was conducted using the LEM, and the Morgenstern–Price method was chosen to study the optimization function. This method was preferred to analyze the slope stability because it satisfies all the static equilibrium requirements [19].

2.1 Geometry and input parameters:

The yield stress in the Mohr–Coulomb model is a function of the major and minor principal stresses, whereas the intermediate principal stress does not affect failure. Consequently, this model was considered suitable and was employed for data analysis. Table 1 shows the physical and mechanical parameters of the soil model for Section 7 at 69.6 km and Section 8 at 70.37 km. Fig. 3 shows the geotechnical model for Sections 7 and 8

Table 1 input data and the values and description layers and soil for Section 7 and 8 [29][30].

Soil description	Thickness m	E kN/m^2	γ kN/m^3	C kN/m^2	Ø degree	υ	K_o
a. Section (7) at 69.6 km							
Asphalt	0.10	5400×10^3	25	-	-	0.35	0.5
Base (Crushed Gravel)	0.15	250×10^3	21	30	43	0.35	0.3
Subbase (Crushed Gravel)	0.25	120×10^3	22	20	44	0.35	0.36
Subgrade (Clay)	2	38×10^3	17.9	0.8	19	0.45	0.67
Soil (Clay)	3	36.5×10^3	18	2.5	19	0.45	0.67
b. Section (8) at 70.37 km							
Asphalt	0.1	5400×10^3	25	-	-	0.35	0.5
Base (Crushed Gravel)	0.15	250×10^3	21	30	43	0.35	0.3
Subbase (Crushed Gravel)	0.25	120×10^3	22	20	44	0.35	0.36
Subgrade (Clay)	2	38×10^3	17.9	0.8	21.4	0.45	0.64
Soil (Clay)	3	34.5×10^3	18.4	0.8	19.4	0.45	0.67
Soil (Medium clay)	4	31×10^3	17.4	24.8	0	0.45	1

E: elasticity modulus, **γ:** volume weight, **C**: effective cohesion, **ϕ:** angle of internal friction, **υ:** Poisson's ratio , and **K_0:** Earth pressure coefficient at rest
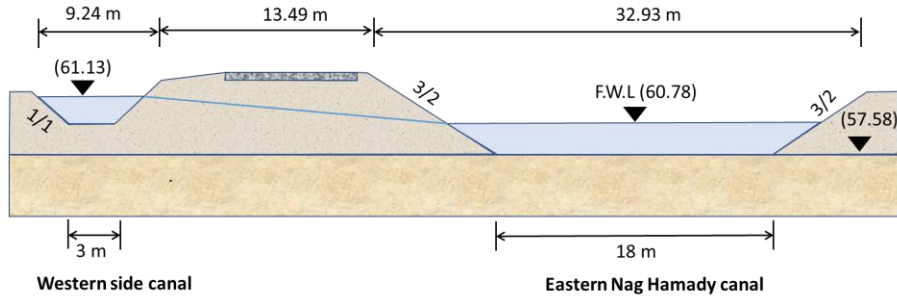
a. Section 7 at 69.6 km
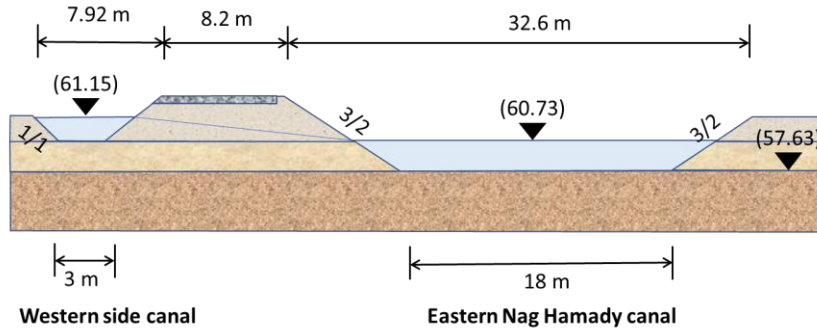
b. Section 8 at 70.37 km

Fig. 3 Detailed cross sections of Sections 7 and 8 [29].

2.2 Surcharge load

The surcharge loads were applied to the models in this study by using a load of 30 kPa/m as an extreme case (a fully loaded concrete truck) [31].

2.3 Seismic coefficient

Horizontal and vertical pseudo-static (seismic) coefficients, K_h and K_v are used to calculate the horizontal and vertical forces induced by a potential earthquake, as illustrated in Fig. 4. Those forces are then added to the overall equilibrium calculation for each of the slices that make up the failure surface, making them more stable.
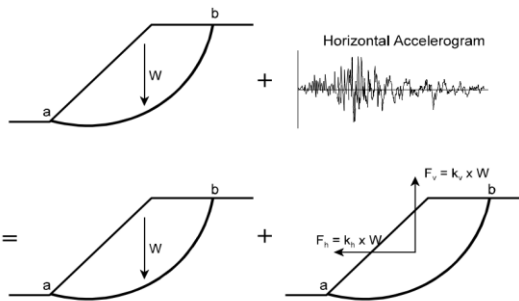
Fig. 4 Pseudostatic analysis approach [32].

The most important aspect of pseudo-static stability analysis is choosing an appropriate seismic coefficient. The horizontal seismic coefficient values recommended by Terzaghi for different earthquake conditions are shown in Table 2.

Table 2 Recommended Horizontal Seismic Coefficient [33].

Horizontal seismic coefficient, K_h	Description
0.1	Severe earthquakes
0.2	Violent, destructive earthquakes
0.5	Catastrophic earthquakes

The horizontal seismic coefficient value was applied to the models in this study is 0.1 because Egypt is considered an area of relatively low to moderate seismicity [34].

The vertical seismic coefficient was neglected because it reduces both the driving force and the resisting force; thus, it has less influence on the factor of safety [35].

2.4 Soil nail

The specified bar capacity is 300 kN with a bar safety factor of 1.5 and 1.5 m spacing in the horizontal

direction in unity. Consequently, the maximum load applied is 133.33 kN (300/1.5/1.5). The specified bond skin friction is 100 kN/m^2 with a bond safety factor of 1.5. Consequently, the bond resistance applied is 44.44 kN/m (100/1.5/1.5). The diameter of the grouted section in contact with the soil (bond diameter) is 0.318 m [4], [36], [37].

Fig. 5 shows the distribution of soil nails in the road embankment. In this research, we will study the effect of the change in the nail length, soil nail inclination, and number of rows of soil nails using the optimized LEM.

a. Three rows of nails

b. Four rows of nails

C. Five rows of nails

b. Six rows of nails
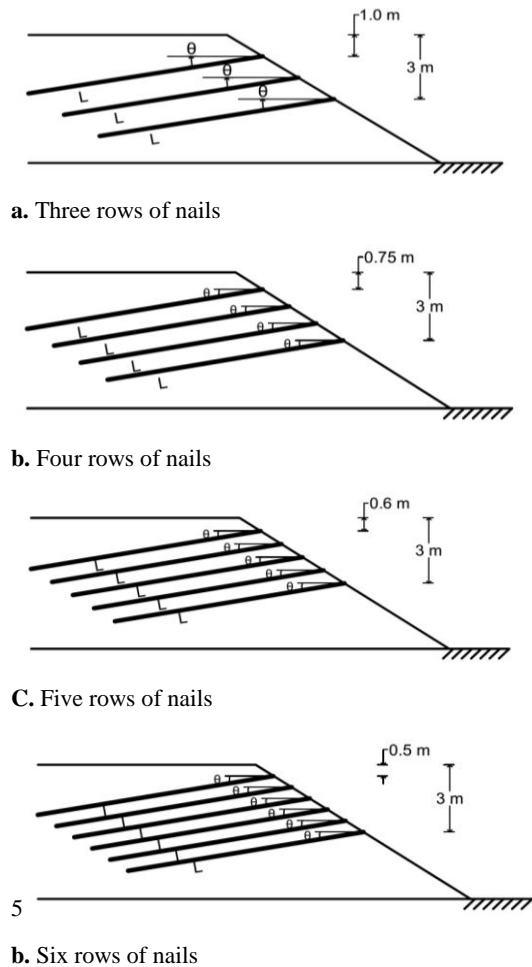
Fig. 5 The nail support systems

L: Length of nail and **θ:** Soil nail inclination (to the horizontal)

2.5   Optimization function in SLOPE/W

Table 3 lists the parameters we recommended in the optimization function in our cases.

Table 3 Input parameters for the optimization function in SLOPE/W.

Parameter	input value	Limits
No. of iterations	2000	--
Convergence tolerance for the FOS	10^{-7}	--
No. of starting points	8	> 0
No. of ending points	16	$\geq$ starting points
No. of finished passes per point insertion		--
Slip surface concave angle on the driving side, βd	5°	$0° < βd \leq 30°$
Slip surface concave angle on the resisting side, βr	1°	$0° < βr \leq 10°$

The optimization process in SLOPE/W begins by dividing the critical trial slip surface into several straight-line segments, as shown in Fig. 5. The number of endpoints determines the number of line segments, which; we recommend a value of 16. The optimum slip surface is determined by the user's choice of starting point or the recommended value of 8 and the number of ending points. This determines to the extent to which the optimized slip surface can deviate from the circular slip surface from which it was constructed. The first vertex is relocated when the slip surface enters the ground surface. This point is moved randomly until the minimum local FOS is found. The number of completed passes per point insertion controls how many random walks are generated for each vertex, for which we recommend a value of 1.

The user must evaluate the plausibility of the obtained slip surface. In SLOPE/W, users may specify the maximum concave angles that the software should allow for the driving and resisting masses, respectively. This parameter is the only known limitation on the shape of the optimized slip surface. The maximum concave angle cannot be set to 0°, but most slip surfaces with distinct concave angles seem peculiar and kinematically incorrect. Fig.6 shows an example of a composite slip surface obtained by optimizing a circular slip surface.

a. Traditional   **b.** Optimized
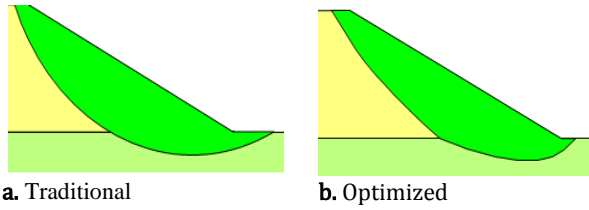
Fig. 6 Traditional and optimized slip surface [22].

3. Results and discussion

Tables 4 and 5 list the FOS values of slope stability determined using the traditional and optimized LEM when soil nailing is used to stabilize the in Sections 7 and 8 for varying nail lengths, soil nail inclination, and number of soil nail rows in the vertical direction, when the spacing of soil nails in the horizontal direction is 1.5 m.

The soil nails are 8 m long, the FOS values were close despite the increase in the number of rows of soil nails, and the maximum FOS obtained by the optimized LEM was reached when five rows of soil nails were used with 50° soil nail inclination. Figs. 7 and 8 show the shape and position of the slip surface when 8-m-long soil nails were used in five rows with an inclination of 50°.

Table 4 FOS values when soil nailing is used at Section 7 (69.6 km)

L (m)	θ	FOS							
		N = 3 Rows		N = 4 Rows		N = 5 Rows		N = 6 Rows	
		Traditional	Optimized	Traditional	Optimized	Traditional	Optimized	Traditional	Optimized
8	10	0.801	0.771	0.807	0.779	0.814	0.780	0.814	0.788
	20	0.839	0.811	0.841	0.821	0.844	0.823	0.850	0.830
	30	0.871	0.847	0.874	0.850	0.881	0.856	0.883	0.849
	40	0.888	0.862	0.911	0.874	0.913	0.876	0.913	0.872
	50	0.863	0.828	0.874	0.765	0.894	0.767	0.910	0.817
	60	0.740	0.532	0.707	0.526	0.751	0.575	0.719	0.580
10	10	0.910	0.850	0.907	0.847	0.920	0.849	0.924	0.848
	20	0.912	0.897	0.955	0.911	0.966	0.928	0.970	0.931
	30	0.905	0.818	0.969	0.912	1.019	0.962	1.021	0.973
	40	0.888	0.862	0.947	0.890	0.995	0.932	1.038	0.952
	50	0.863	0.828	0.874	0.793	0.894	0.802	0.910	0.817
	60	0.740	0.532	0.724	0.535	0.754	0.575	0.719	0.575
12	10	0.910	0.900	0.980	0.957	1.034	0.965	1.043	0.986
	20	0.912	0.897	0.982	0.940	1.038	0.981	1.089	1.017
	30	0.905	0.885	0.969	0.912	1.023	0.947	1.071	0.978
	40	0.888	0.862	0.947	0.890	0.995	0.932	1.038	0.952
	50	0.866	0.834	0.874	0.793	0.894	0.797	0.910	0.817
	60	0.843	0.541	0.724	0.535	0.754	0.575	0.719	0.575

L: length of soil nail, **N:** number of rows of nails, and **θ:** soil nail inclination (to the horizontal)

Table 5 FOS values when soil nailing is used at Section 8 (70.37 km)

L (m)	θ	FOS							
		N = 3 Rows		N = 4 Rows		N = 5 Rows		N = 6 Rows	
		Traditional	Optimized	Traditional	Optimized	Traditional	Optimized	Traditional	Optimized
8	10	0.986	0.944	1.001	0.960	0.990	0.943	0.995	0.953
	20	1.001	0.977	1.010	0.966	1.017	0.989	1.005	0.973
	30	1.008	0.986	1.013	0.987	1.010	0.987	1.012	0.987
	40	1.012	0.918	1.022	0.995	1.019	0.993	1.019	0.992
	50	0.950	0.820	1.076	0.986	1.078	1.006	1.078	1.002
	60	0.770	0.569	0.834	0.601	0.806	0.554	0.798	0.537
10	10	1.039	0.993	1.053	0.995	1.055	0.993	1.055	0.993
	20	1.088	0.955	1.089	1.027	1.080	1.032	1.088	1.037
	30	1.076	0.926	1.142	1.072	1.158	1.114	1.160	1.115
	40	1.022	0.918	1.101	1.014	1.111	1.017	1.139	1.027
	50	0.943	0.820	1.076	0.986	1.079	0.965	1.081	0.929
	60	0.777	0.569	0.834	0.601	0.806	0.554	0.798	0.620
12	10	1.104	0.985	1.189	1.162	١.١٩٢	1.048	1.213	1.048
	20	1.098	0.955	1.169	1.105	1.211	1.141	1.248	1.162
	30	1.065	0.926	1.142	1.072	١.١٧١	١.٠٩٦	1.190	1.105
	40	1.012	0.918	1.101	1.014	١.١١١	١.٠١٧	1.139	1.027
	50	0.950	0.820	1.076	0.986	١.٠٧٩	٠.٩٦٥	1.081	0.929
	60	0.770	0.569	0.834	0.601	٠.٨٠٦	٠.٥٥٤	0.798	0.537

L: length of soil nail, N: number of rows of nails, and θ: soil nail inclination (to the horizontal)
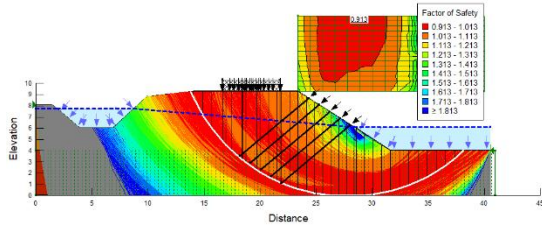
a. Traditional
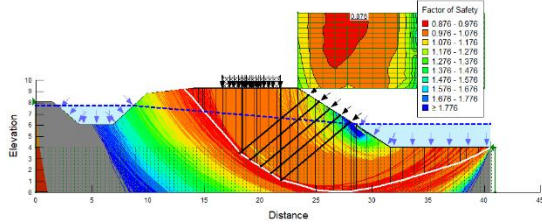
b. Optimized

Fig. 7 Shape and position of slip surface at Section 7 when N = 5, θ =50°, and L = 8 m.
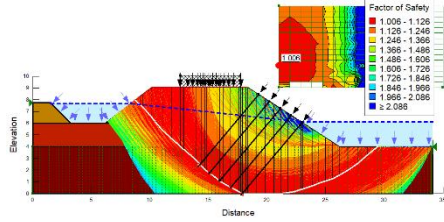
a. Traditional
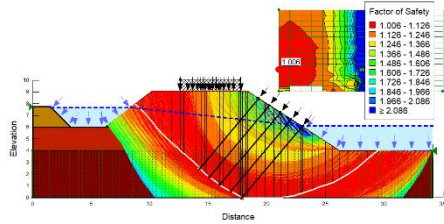
b. Optimized

Fig. 8 Shape and position of slip surface at Section 8 when N = 5, θ =50°, and L = 8 m

When the length of the soil nails was increased to 10 m and the increase in the number of rows was increased to 6, the FOS values increased. Figs. 9 and 10 show the shape and position of the slip surface when 10-m-long using soil nails in six rows with an inclination of 30°.
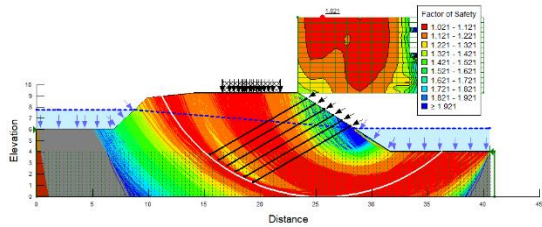
a. Traditional
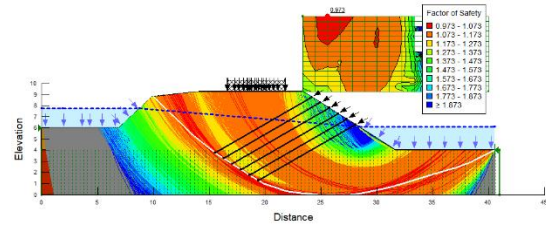
b. Optimized

Fig. 9 Shape and position of slip surface at Section 7 when N = 6, θ = 30°, and L = 10 m.
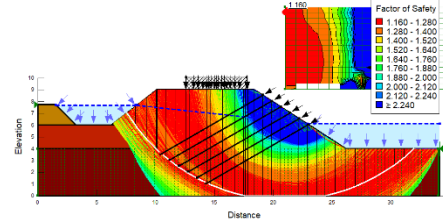
a. Traditional
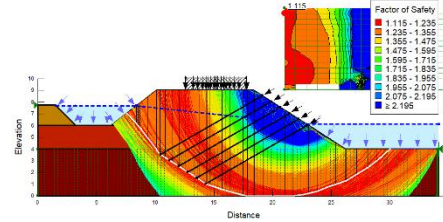
b. Optimized

Fig. 10 Shape and position of slip surface at Section 8 when N = 6, θ = 30°, and L = 10 m.

When the soil nails were 8 m and 10 m long, the slip surface occurred beyond the soil nails, indicating that the length of the nails was not sufficient to resist the slip surface. When the length of the soil nails was increased to 12 m, the nail force reached its maximum of 44.44 kN. Figs. 11 and 12 show the shape and position of the slip surface when 12-m-long soil nails were used in six rows with an inclination of 20°.
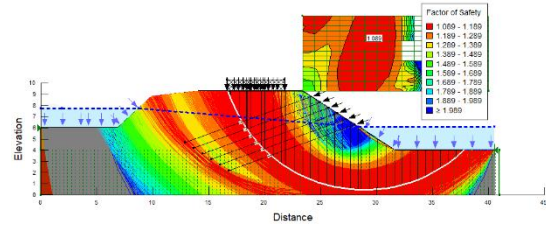
a. Traditional
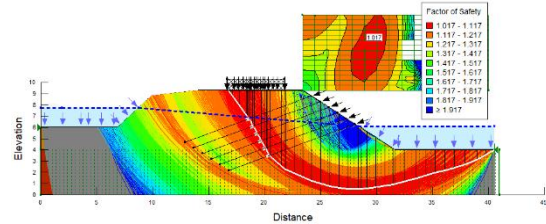
b. Optimized

Fig. 11 Shape and position of slip surface at Section 7 when N = 6, θ = 20°, and L = 12 m

a. Traditional
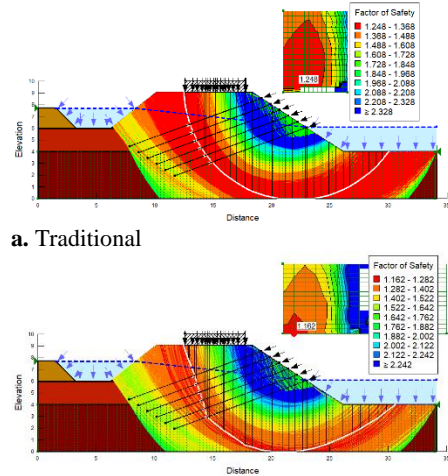
b. Optimized
Fig. 12 Shape and position of slip surface at Section 8 when N = 6, θ = 20°, and L = 12 m.

The results indicate that all of the soil nails have achieved their maximum nail force, the slip surface occurs through all soil nails, and that the length of the nails was sufficient to resist the slip surface. Tables 6 and 7 show the maximum soil nail force in the previous cases. When the length of the soil nails was 8 or 10 m, the soil nail force did not reach the maximum designed force, which was 44.44 kN. That indicates that the length of the soil nails was insufficient, whereas for a length of 12 m, the soil nail force reached the maximum designed force, which shows an increase in the FOS of slope stability with increasing soil nail length.

Table 6 Maximum nail force when soil nailing is used at Section 7 (69.6 km)

N	θ	L	Maximum nail force (kN)	
			Traditional	**Optimized**
5	40	8	0	0
6	30	10	1.89	0.145
6	20	12	44.44	44.44

L: length of soil nail, **N:** number of rows of nails, and **θ:** soil nail inclination (to the horizontal)

Table 7 Maximum nail force when soil nailing is used at Section 8 (70.37 km)

N	θ	L	Maximum nail force (kN)	
			Traditional	**Optimized**
5	50	8	0	0
6	30	10	8.658	0.199
6	20	12	44.44	44.44

L: length of soil nail, **N:** number of rows of nails, and **θ:** soil nail inclination (to the horizontal)

According to the Federal Highway Administration [33], [34], the FOS total slope stability is 1.35. It was noticed that the maximum values of the safety factor in Sections 7 and 8 were 1.017 and 1.162, respectively, when the length of the soil nails was 12 m with 20° soil nail inclination in six rows of soil nails. The value of the safety factor in Sections 7 and 8 were not sufficient for total slope stability, so it was necessary to further increase the soil stability. We attempted to reduce the horizontal spacing between the soil nails to 0.5 m instead of 1.5 m.

It was found that when the length of the soil nails was 12 m with a 20° inclination in six rows of soil nails, the FOS was increased from 1.017 to 1.477. The position and shape of the slip surface also differed with the decrease in the horizontal spacing between the soil nails to 0.5 m. As well, when the horizontal spacing between the soil nails was reduced to 0.5 m and the inclination was 30°, the FOS increased from 0.978 to 1.339. Fig. 13 shows the FOS values and the shape and position of the slip surface when the horizontal spacing is reduced to 0.5.

a. θ = 20°, FOS = 1.477
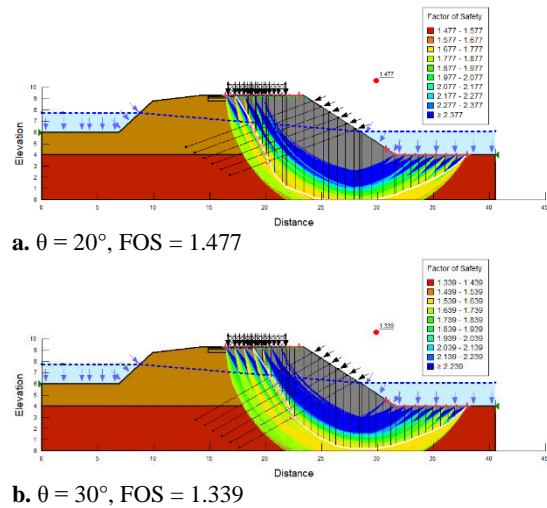
b. θ = 30°, FOS = 1.339
Fig. 13 Shape and position of slip surface at Section 7. N = 6, θ = 20° and 30°, and L = 12 m when spacing is 0.5 m.

Fig. 14 shows Section 8 when the length of the soil nails was 12 m with 20° inclination in six rows. The FOS increased from 1.162 to 1.418 when the horizontal spacing between the soil nails was reduced to 0.5 m instead of 1.5 m. As well, at a soil nail

inclination of 30°, the FOS increased from 1.105 to 1.131, similar to the results of Section 7.
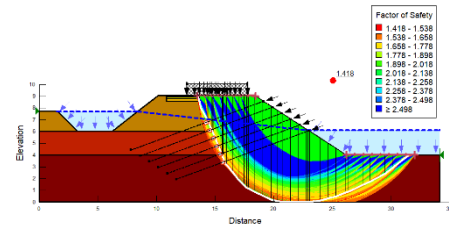
a. θ = 20°, FOS = 1.418
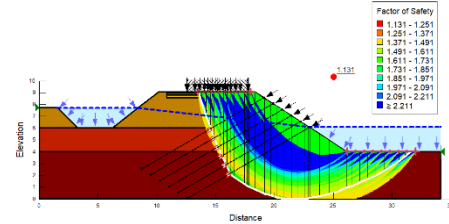
b. θ = 30°, FOS = 1.131

Fig. 14 Shape and position of slip surface at Section 8. N = 6 , θ = 20° and 30°, and L = 12 m when spacing is 0.5 m.

Tables 7 and 8 lists the FOS values of slope stability determined when the horizontal spacing is reduced to 1 m and 0.5 m.

Table 7 FOS values when decreased horizontal spacing between nails in Section 7 (69.6 km).

θ	FOS		
	S = 1.5 m	S = 1 m	S = 0.5 m
20	1.017	1.120	1.477
30	0.978	1.057	1.339

Θ: soil nail inclination (to the horizontal) and **S** = the horizontal spacing between the soil nails.

Table 8 FOS values when decreased horizontal spacing between nails in Section 8 (70.37 km).

θ	FOS		
	S = 1.5 m	S = 1 m	S = 0.5 m
20	1.162	1.225	1.418
30	1.105	1.114	1.131

Θ: soil nail inclination (to the horizontal) and **S** = the horizontal spacing between the soil nails.

According to the results, it is possible to use the optimization function to obtain more accurate the FOS values and more realistically determine the position and shape of the slip surfaces. When the available input parameters are less advanced, this will aid industrial users and geotechnical engineers. The Morgenstern–Price approach is highly regarded by industry users for its usability and practicality. The LEM is much simpler to apply, requires less effort, thus saving time when establishing a slope model.

4. Conclusion

This study examined the effect of soil nailing on the applicability of optimized mathematical models of the slope stability of road embankments under traffic load. Soil nailing was studied in terms of inclination, spacing, and length. Based on the results of this study, the following conclusions can be drawn

- Based on the analysis results from all cases covered by this study, LEM's optimized method enhanced the value of the safety coefficient and modeled the slip surface's shape and position in a more realistically.
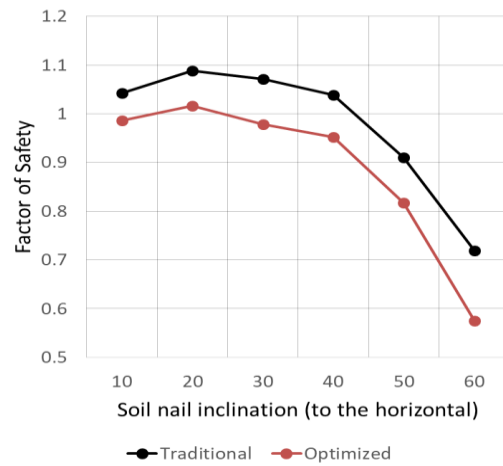
a. Section 7
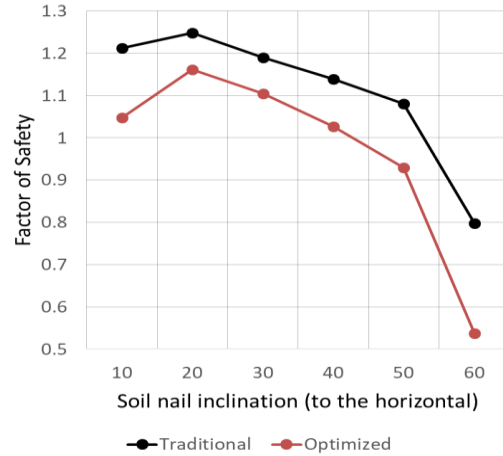
b. Section 8
Fig. 15 The safety factors when using soil nailing were as follows: number of rows = 6, soil nail inclination (to the horizontal) = (10°, 20°, 30°, 40°, 50°, and 60°), and length of soil nail = 12 m.

- The soil nails exhibit obvious reinforcing effects on the slope stability. When the length of the soil nails was 8 or 10 m, the soil nail force did not

reach the maximum designed force, which is 44.44 kN. This indicates that the length of the soil nails was not sufficient, whereas the maximum design force was reached when soil nails with a length of 12 m were used. This demonstrates the increase in the FOS of slope stability with the increasing length of soil nails.
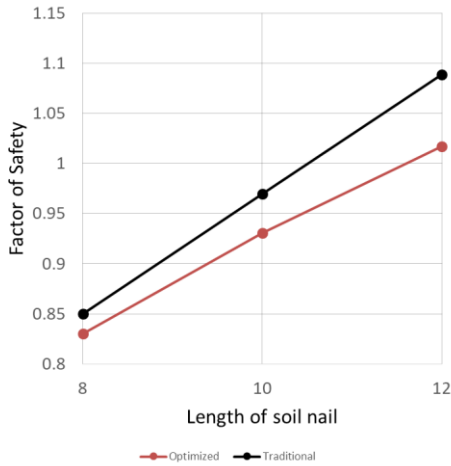
a. Section 7
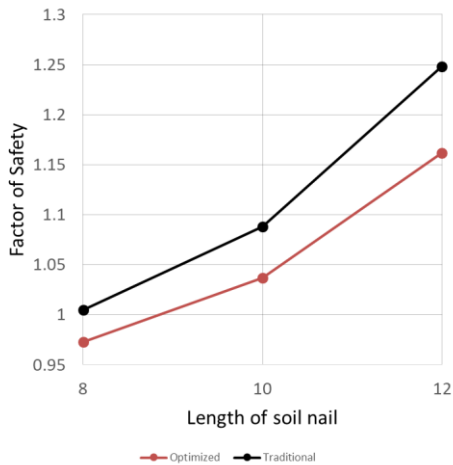
b. Section 8

Fig. 16 The safety factors when using soil nailing were as follows: number of rows = 6, soil nail inclination (to the horizontal) = 20°, and length of soil nail = (8 m, 10 m, and 12 m).

- Additionally, when the number of rows increased, the FOS value also increased.
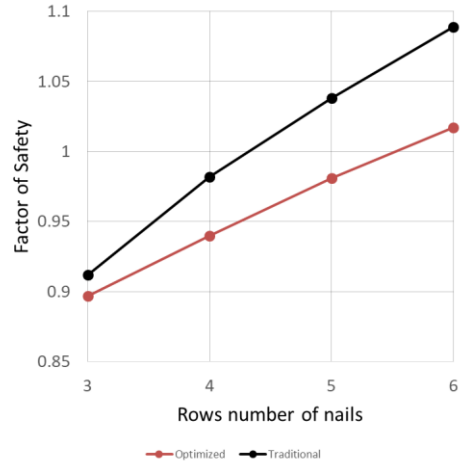
a. Section 7
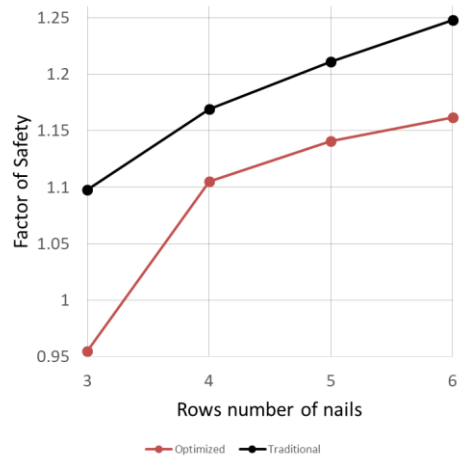
b. Section 8

Fig. 17 The safety factors when using soil nailing were as follows: number of rows = (3, 4, 5, 6), soil nail inclination (to the horizontal) = 20°, and length of soil nail = 12 m.

- When the length of the soil nails was 12 m with 20° soil nail inclination in six rows of soil nails, the value of the safety factor was increased when the horizontal spacing between the soil nails was reduced to 0.5 m instead of 1.5 m. As well, at an inclination of 30°, the value of the safety factor increased. Therefore, the proper inclination of the soil nails in this study was 20°.

Finally, we recommended that for future studies

- Study seepage forces because, in such case of embankment between two canals, seepage force is important.
- Study the effect of variation in soil properties on the applicability of optimized mathematical models of slope stability.

References

[1] C. Liu and U. Hounsa, "Analysis of road embankment slope stability," *Open J. Civ. Eng.*, vol. 08, pp. 121–128, 2018, doi: 10.4236/ojce.2018.82010.

[2] P. Sharma, "Theoretical analysis of soil nailing: design, performance and future aspects," *Int. J. Eng. Res. Gen. Sci.*, vol. 3, pp. 644–653, 2015.

[3] J. Liu, K. Shang, and X. Wu, "Stability analysis of soil nailing supporting structure based on system failure probability method," in *Geotechnical Special Publication*, 2014, pp. 39–47, doi: 10.1061/9780784478523.006.

[4] A. Quansah, "Optimum design analysis of a nailed slope based on limit equilibrium methods: case study - Cluj-Napoca landslide," *J. Civ. Eng. Res.*, vol. 8, pp. 49–61, 2018, doi: 10.5923/j.jce.20180803.01.

[5] A. Garg, A. Garg, K. Tai, and S. Sekharan, "An integrated SRM-multi-gene genetic programming approach for prediction of factor of safety of 3-D soil nailed slopes," *Eng. Appl. Artif. Intell.*, vol. 30, 2014, doi: 10.1016/j.engappai.2013.12.011.

[6] Y. Kim, S. Lee, S. Jeong, and J. Kim, "The effect of pressure-grouted soil nails on the stability of weathered soil slopes," *Comput. Geotech.*, vol. 49, pp. 253–263, 2013, doi: 10.1016/j.compgeo.2012.12.003.

[7] B. Leshchinsky, "Limit equilibrium and limit analysis: comparison of benchmark slope stability problems," *J. Geotech. Geoenvironmental Eng.*, 2015, doi: 10.1061/(ASCE)GT.1943-5606.0001347.

[8] H. Khabbaz, B. Fatahi, and C. Nucifora, "Finite element methods against limit equilibrium approaches for slope stability analysis," 2012.

[9] W. Fellenius, *Erdstatische Berechnungen mit Reibung und Kohäsion*. Berlin: Ernst Verlag, 1927.

[10] A. W. Bishop, "The use of the slip circle in the stability analysis of slopes," *Geotechnique*, vol. 5, no. 1, pp. 7–17, 1955.

[11] A. W. Bishop and N. Morgenstern, "Stability coefficients for earth slopes," *Geotechnique*, vol. 10, no. 4, pp. 129–153, 1960.

[12] N. Janbu, "Stability analysis of slopes with dimensionless parameters.," Harvard University, Cambridge, 1954.

[13] N. Janbu, "Earth pressure and bearing capacity calculations by generalized procedure of slices," *4th Int. Conf. Soil Mech. Found. Eng.*, vol. 2, pp. 207–212, 1957.

[14] N. Janbu, "slope stability computations," *Embankment-Dam Eng*, pp. 47–86, 1973.

[15] E. Spencer, "A method of analysis of the stability of embankments assuming parallel inter-slice forces," *Geotechnique*, vol. 17, pp. 384–386, 1967.

[16] S. Sarma, "Stability analysis of embankments and slopes," *Géotechnique*, vol. 23, p. 423, 1973, doi: 10.1061/AJGEB6.0000903.

[17] N. R. u Morgenstern and V. E. Price, "The analysis of the stability of general slip surfaces," *Geotechnique*, vol. 15, no. 1, pp. 79–93, 1965.

[18] S. Atashband, "Evaluate reliability of morgenstern--price method in vertical excavations," in *Numerical Methods for Reliability and Safety Assessment: Multiscale and Multiphysics Systems*, S. Kadry and A. El Hami, Eds. Cham: Springer International Publishing, 2015, pp. 529–547.

[19] J. M. Duncan, S. G. Wright, and T. L. Brandon, *Soil strength and slope stability*. John Wiley \& Sons, 2014.

[20] I. Boudjema and S. Djilali, "Turing-Hopf bifurcation in Gauss-type model with cross diffusion and its application," *Nonlinear Stud.*, vol. 25, pp. 665–687, 2018.

[21] H. M. Shiferaw, "Study on the influence of slope height and angle on the factor of safety and shape of failure of slopes based on strength reduction method of analysis," *Beni-Suef Univ. J. Basic Appl. Sci.*, vol. 10, no. 1, p. 31, 2021, doi: 10.1186/s43088-021-00115-w.

[22] GEO-SLOPE International Ltd, *Stability Modeling with SLOPE / W*, no. June. Alberta, Canada: GEO-SLOPE International Ltd, 2015.

[23] V. Greco, "Efficient monte carlo technique for locating critical slip surface," *J. Geotech. Eng.*, vol. 122, pp. 517–525, 1996, doi: 10.1061/(ASCE)0733-9410(1996)122:7(517).

[24] K. Pandit, S. Sarkar, and M. Sharma, "Optimization techniques in slope stability analysis methods," in *Advances in Natural and Technological Hazards Research*, 2018.

[25] A. H. Gandomi, A. R. Kashani, M. Mousavi, and M. Jalalvandi, "Slope stability analysis using evolutionary optimization techniques," *Int. J. Numer. Anal. Methods Geomech.*, vol. 41, no. 2, pp. 251–264, 2017, doi: https://doi.org/10.1002/nag.2554.

[26] A. M. Rashad, M. D. Hashem, A. M. Abdelhamed, and T. E. Mahmoud, "Optimized numerical models of slope stability of roads embankment using limit equilibrium method," in *2nd International Conference on Civil Engineering: Recent Applications and Future Challenges*, 2021, pp. 318–329.

[27] A. Husein Malkawi, W. Hassan, and S. Sarma, "Global search method for locating general slip surface using monte carlo techniques," *J. Geotech. Geoenvironmental Eng. - J Geotech. Geoenviron. Eng*, vol. 127, 2001, doi: 10.1061/(ASCE)1090-0241(2001)127:8(688).

[28] J. Gustafsson, "Applicability of Optimised Slip Surfaces Evaluation of a software's optimisation

function for generating composite slip surfaces, applied on stability analysis of clay slopes," Chalmers University of Technology, 2014.

[29] Mohamed A. Ashour, M. H. Hussein, and Mahmoud Enieb Osman, "Factors affecting the stability of highway side slopes case study: roads adjacent water ways in upper Egypt," vol. 57, no. 1, pp. 11–16, 2007.

[30] M. D. Hashem, A. M. Abu-Baker, and M. D. Hashem, "Numerical modeling of flexible pavement constructed on expansive soils," *Eur. Int. J. Sci. Technol.*, vol. 2, no. 10, pp. 19–34, 2013.

[31] L. Larsson, "Slope Stability Evaluation from a RiskManagement Perspective: Case Study: the Slussen project in Stockholm." 2018.

[32] C. Melo and S. Sharma, "Seismic coefficients for pseudostatic slope analysis," 2004.

[33] K. Terzaghi, "Mechanism of landslides," 1950.

[34] A. Badawy, I. Korrat, H. Mahmoodi, and H. Gaber, "Update earthquake risk assessment in Cairo, Egypt," *J. Seismol.*, vol. 21, 2017, doi: 10.1007/s10950-016-9621-5.

[35] P. Sultana and S. Hazari, *Comparative Study of Soil Slopes Using Static and Pseudo-Static Approaches*. 2014.

[36] S. Alsubal, I. Harahap, and N. Babangida, "A typical design of soil nailing system for stabilizing a soil slope: case study," *Indian J. Sci. Technol.*, vol. 10, 2017, doi: 10.17485/ijst/2017/v10i4/110891.

[37] S. Dewedree and S. N. Jusoh, "Slope stability analysis under different soil nailing parameters using the SLOPE/W software," *J. Phys. Conf. Ser.*, vol. 1174, p. 12008, Feb. 2019, doi: 10.1088/1742-6596/1174/1/012008.

[38] C. A. Lazarte, V. Elias, P. J. Sabatini, and R. D. Espinoza, "Geotechnical Engineering Circular No. 7 - Soil Nail Walls." 2003, [Online]. Available: https://rosap.ntl.bts.gov/view/dot/50250.

[39] C. A. Lazarte, H. Robinson, J. E. Gomez, A. Baxter, A. Cadden, and R. R. Berg, "Geotechnical Engineering Circular No. 7 Soil Nail Walls - Reference Manual." 2015, [Online]. Available: https://rosap.ntl.bts.gov/view/dot/40556.